



Contents lists available at ScienceDirect

Tectonophysics

journal homepage: www.elsevier.com/locate/tecto

Field observations of geological effects triggered by the January–February 2014 Cephalonia (Ionian Sea, Greece) earthquakes

Sotirios Valkaniotis^a, Athanassios Ganas^{b,*}, George Papathanassiou^c, Marios Papanikolaou^b

^a 9 Koronidos Str., 42100 Trikala, Greece

^b Institute of Geodynamics, National Observatory of Athens, 11810 Athens, Greece

^c Department of Geology, Aristotle University of Thessaloniki, Greece

ARTICLE INFO

Article history:

Received 8 March 2014

Received in revised form 6 May 2014

Accepted 12 May 2014

Available online xxxxx

Keywords:

Cephalonia

Earthquake

Liquefaction

Strike-slip

Fault

Greece

ABSTRACT

On Jan. 26 and Feb 3, 2014 Cephalonia Island, Ionian Sea, Greece, was struck by two strong, shallow earthquakes (NOA local magnitudes M_L 5.8 and M_L 5.7, respectively). The earthquakes ruptured two sub-parallel, strike-slip faults, with right-lateral kinematics. During both earthquakes, ground-shaking phenomena such as liquefaction, road failures, rock falls, small/medium size landslides and stonewall failures were widespread all over the western part of the island. No primary fault surface ruptures were observed, however one patch of the rupture of the second event may have nearly reached the surface, because of the abundance of surface cracks with cm-size offsets mapped in the field in north Paliki Peninsula. Liquefaction phenomena were mainly triggered in reclaimed lands in the waterfront areas of Argostoli and Lixouri inducing structural damages to quays, sidewalks and piers. We also present evidence for liquefaction-induced ground disruption in the recently constructed marina of Argostoli, which is situated at the opposite (eastern) shore to the town.

© 2014 Elsevier B.V. All rights reserved.

1. Introduction

Ionian Sea (western Greece) is a plate-boundary region of high seismicity and complex tectonics, dominated by frequent earthquake activity along the right-lateral Cephalonia Transform Fault (CTF). Cephalonia has been repeatedly subjected to strong ground shaking due to the proximity of the island to CTF (Fig. 1; Louvari et al., 1999; Sachpazi et al., 2000; Scordilis et al., 1985). The 100-km long fault zone accommodates the relative motion of the Apulia (Africa) and Aegean (Eurasia) lithospheric plates, and has a GPS slip-rate bracketed between 10 and 25 mm/yr (e.g., Pérouse et al., 2012). The most recent large CTF events include the Jan. 17, 1983 ($M = 6.8$ global CMT catalogue; Scordilis et al., 1985) and the Aug. 14, 2003 ($M = 6.2$ global CMT catalogue; Papathanassiou et al., 2005). Two strong earthquake events, with M_L (NOA) 5.8 and M_L (NOA) 5.7, occurred on Jan. 26, 2014 13:55 UTC and Feb. 3, 2014 03:08 UTC, respectively, onshore the island of Cephalonia (Fig. 1; Ganas et al., 2014; Karastathis et al., 2014) inducing extensive structural damages and environmental effects, mainly in the western and central parts. According to the National Observatory of Athens, Institute of Geodynamics (NOA; <http://www.gein.noa.gr>) the epicentre of the first event (Fig. 1; NOA web report, 2014) was located

near the town of Argostoli (the capital), while the second one was located to the north of village Livadi (Fig. 2; Paliki Peninsula). Both earthquakes were shallow (relocated by Karastathis et al., 2014) and occurred on near-vertical, strike-slip faults with dextral sense of motion (NOA Moment Tensor solutions available online at <http://bbnet.gein.noa.gr/HL/seismicity/moment-tensors>), in response to ENE–WSW horizontal strain in central Ionian Sea (Ganas et al., 2013a; Hollenstein et al., 2008).

This paper is the outcome of three field surveys that took place immediately after the occurrence of both earthquakes (Jan. 28–31, 2014; Feb. 4–6, 2014 & Feb. 6–9, 2014) and thus, we were able to timely report the triggered geo-environmental effects (liquefaction, slope failures etc.). In the following pages, a detailed map and brief description of the earthquake-induced failures is presented while more information will be published after data processing.

2. Field observation of geological effects

During both events, the majority of earthquake-related phenomena were liquefaction, road failures, rock falls and small landslides. These phenomena were widespread in the Paliki peninsula and the area around Argostoli Bay (Fig. 2). In the northern and eastern parts of the island only few isolated rock falls and landslides in loose materials were observed. It must be noted that most environmental effects were created after the first event in Jan. 26 and were reactivated one week later in the second (Feb. 3) event.

* Corresponding author.

E-mail addresses: valkaniotis@yahoo.com (S. Valkaniotis), aganas@noa.gr (A. Ganas), gpapatha@geo.auth.gr (G. Papathanassiou), marios_pap@yahoo.com (M. Papanikolaou).

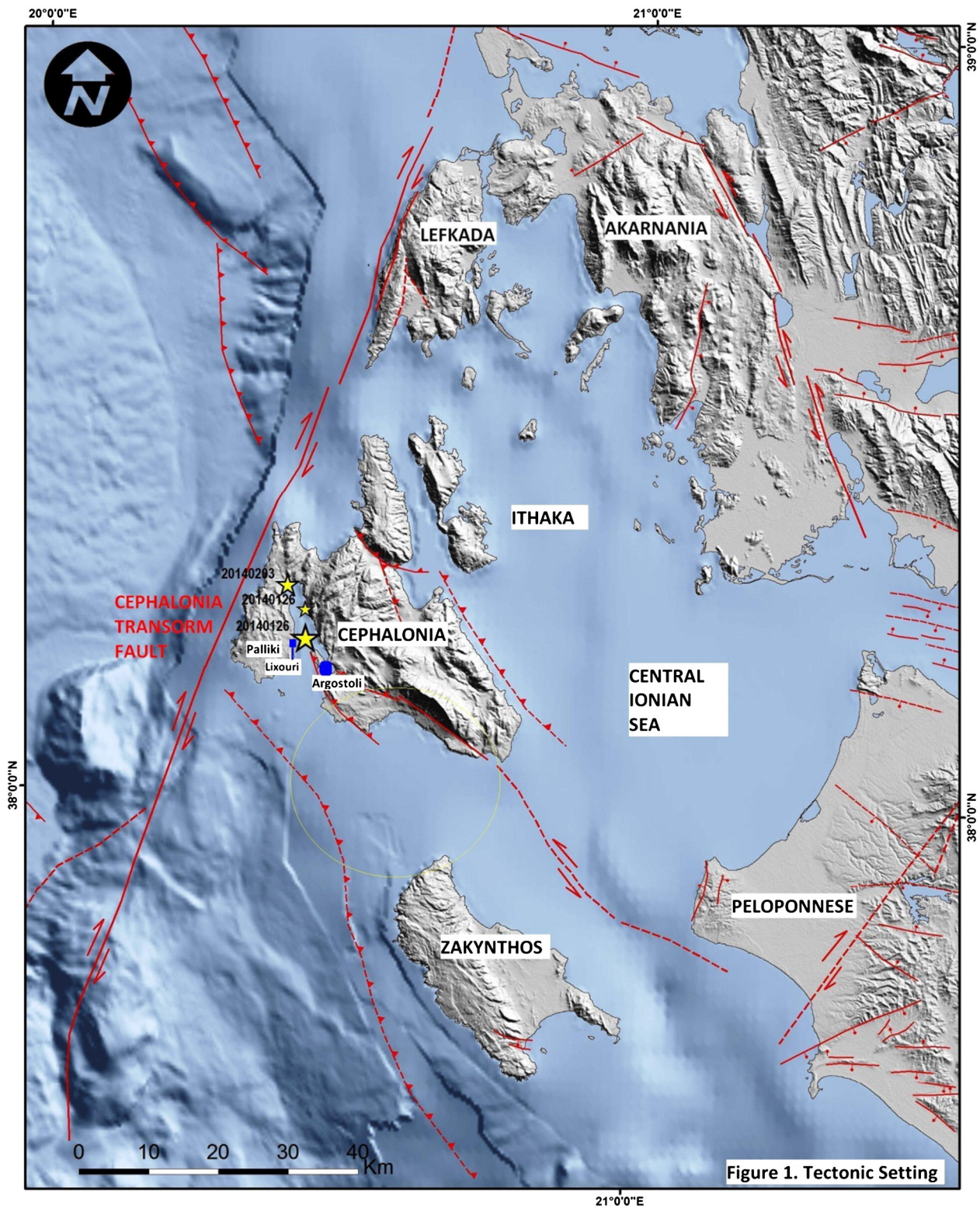


Fig. 1. Location map showing the epicentres (yellow stars) of the two mainshocks and one aftershock of Jan. 26, 2014 at 18:45 UTC. Red lines are active faults (dashed are inferred; from Ganas et al., 2013b), arrows indicate sense of motion. (For interpretation of the references to colour in this figure legend, the reader is referred to the web version of this article.)

2.1. Ground cracks

Field observations of ground cracks were made at the central/north part of Paliki peninsula (Figs. 3 and 4). The southernmost locality of their observation was the church in the centre of Skineas village (Fig. 3) where a continuous crack with minor (<1 cm) dextral

displacement was mapped for a length of 10 m. Measurement of the crack's strike shows a N20°–30°E orientation. On the road leading from Atheras village to Porto Atheras beach (Fig. 2), we observed two localities with cracks: first a fracture near a Quaternary (?) fault plane (with attributes N137°E/70°; dip direction, dip angle; see NE-striking fault to the east of the crack number 53 in Figs. 2 & 3) with a dextral



Fig. 2. Geological map of western Cephalonia showing the distribution of earthquake-induced geological effects. Geological formations and faults are modified from Lekkas et al. (2001).

sense of movement and in the second one, few metres downslope, there was a landslide of brecciated material, together with cracks (showing dextral sense of motion) on the road surface.

A locality of several ground displacement observations was about halfway the road leading from Atheras to Livadi (Figs. 2 and 3). In two localities along this road three cracks ruptured the road after the Jan.

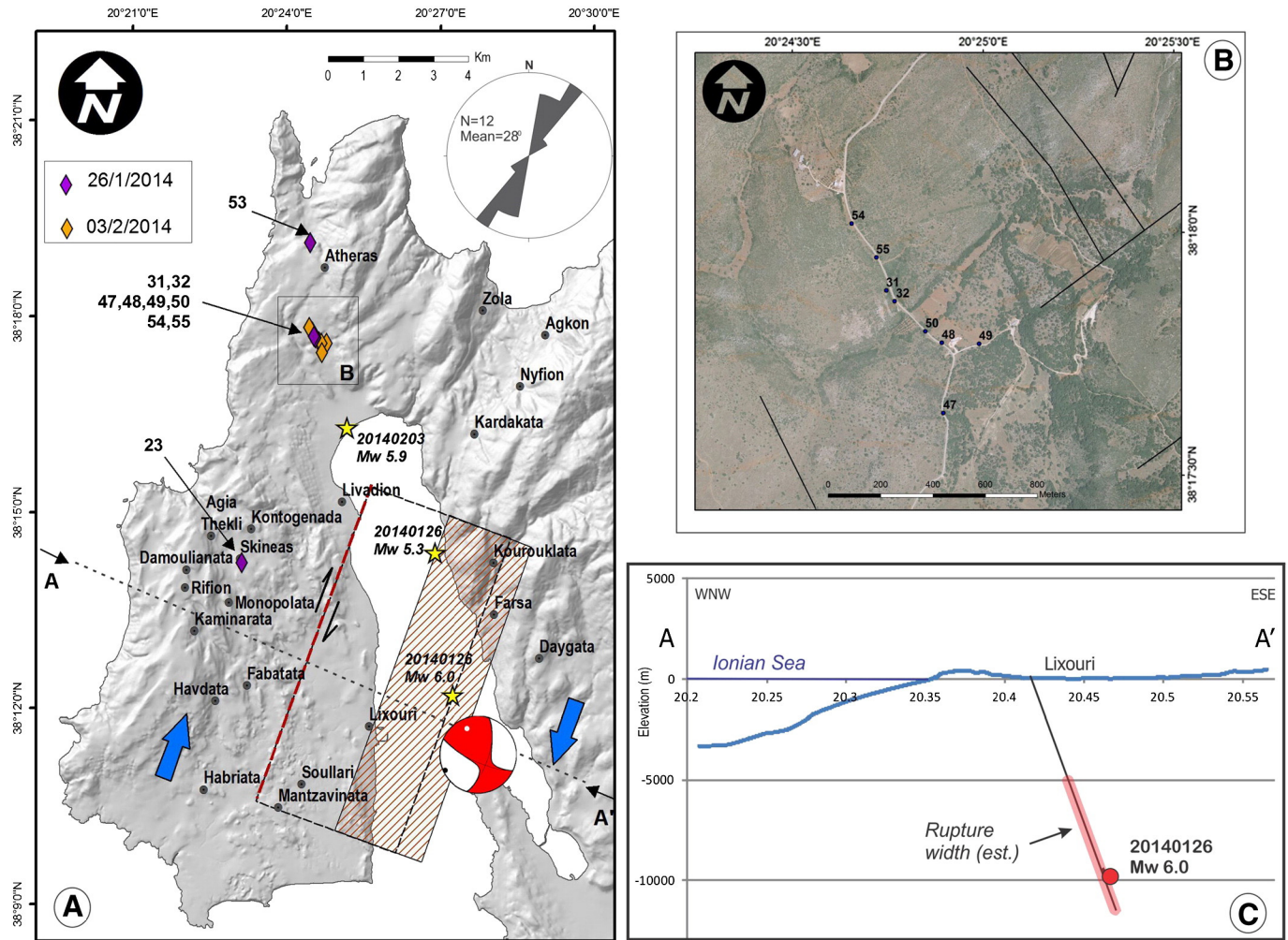


Fig. 3. A) Relief map of Paliki Peninsula with surface projection of Jan. 26, 2014 seismic fault (straight red line; fault attitude $18^{\circ}/67^{\circ}/164^{\circ}$ strike/dip/rake, from NOA MT solution). Yellow star symbols indicate epicentre location of the two main events and the largest aftershock. Rhomb symbol indicate locality with structural measurements. Rose diagram displays azimuth of ground cracks mapped on the field (Paliki peninsula) which is roughly parallel to the strike of CTF and the NNE nodal plane of the MT solutions. B) Air-photo of the area with observed ground cracks between Atheras and Livadi. C) WNW–ESE cross-section with inferred positions of the Jan. 26, 2014 high-angle fault and estimated rupture width. Letters A and A' on the map indicate end points of section. Numbers refer to localities in Table 1. (For interpretation of the references to colour in this figure legend, the reader is referred to the web version of this article.)

26, 2014 earthquake with azimuth (strike) of $N30^{\circ}E$ – $N50^{\circ}E$ (Fig. 4A). The road is constructed directly on a karstified limestone, with a thin red soil cover locally reaching 5–10 cm depth. After the Feb. 3, 2014 earthquake, the same cracks showed signs of further displacement and newer fractures were found in five (5) places along a ~600 m stretch of the road. Measurement of the fractures shows a similar orientation ($N15^{\circ}E$ – $N41^{\circ}E$). Additional cracks were mapped across a dirt road to the east (number 49 on Fig. 3, possible extension of number 47 crack; see air-photo detail in Fig. 3B). This locality shows a clear and fresh rupture of the bedrock with a dextral horizontal displacement of 2–4 cm (Fig. 4B). These limestone breaks didn't exist in the pre-Feb. 3rd field investigation, so they are attributed to the Feb. 3, 2014 earthquake. A rose diagram shows that ground cracks mapped on the field (Paliki peninsula) have a mean azimuth of $N28^{\circ}E$ (Fig. 3A), roughly parallel to CTF strike and to NNE–SSW nodal plane of MT solutions.

2.2. Slope failures

The earthquake-induced slope instabilities caused road failures along the road network in the island of Cephalonia. These failures were observed in an area with radius of ~10 km around the epicentre of Jan. 26, 2014 (Fig. 2). The failures were especially severe in the south/central part of Paliki peninsula and in the east coast of Argostoli

Bay, and resulted in days-long closure of these roads for traffic. On the south Paliki, we observed damages on road network, connecting villages on hills with Neogene soft sediments, due to the failure of artificial fills beneath the pavement.

In particular, landslides of small/medium size were widespread in soft Neogene and Quaternary sediments (Fig. 2), but also locally observed in clastic formations of Miocene flysch deposits. One of the most impressive mass-movement phenomena was the Soullari large landslide (Fig. 5), situated NE from the Soullari village in Paliki peninsula. The landslide was activated during the first earthquake (Jan. 26) on homogenous silt/clay Pliocene–Pleistocene sediments, in a small field on top of a hill. Measuring 20 m length and 30 m width, the landslide's initial rupture on the crown was along the pre-existing set of joints (NE–SW direction) and was re-activated after the second event (Feb. 3, 2014; Fig. 5 right). The re-activation was most probably assisted by the presence of rain water in the week following the first earthquake, and caused further movement of the block down-hill, along with a break of the block piece in two smaller ones and collapse of the surrounding scar-walls.

The western coast of Paliki peninsula is an almost continuous steep (150–300 m height) cliff on carbonate formations of Paxoi Zone of the Hellenides. Rock falls and locally loose material flows were observed along parts of the coast from Myrtos beach to the south-west end of



Fig. 4. Field photographs of geological effects: A) Road crack near Atheros village (photo taken Feb. 7, 2014, see point 32 in Fig. 3). B) Post-Feb. 3, 2014 earthquake photo of a crack in bedrock near Atheros (see point 32 on Fig. 3). C) Ground crack (see point 49 in Fig. 3B). D) Road crack (see point 50 in Fig. 3B).

Paliki peninsula and along the steep, east coast of Argostoli Bay. Especially in Myrtos Bay, heavy damaging rock falls rolled along the steep cliffs damaging the roads and even reaching the beach. Limestone blocks reaching 1–2 m rolled down to Atheros village causing damage in few properties. Rock falls were also widespread in the western and central part of the island. Few isolated small rock falls were observed in the northern and eastern part, and along the south cliff of Ainos

Mountain, associated with road cuts in Quaternary loose deposits. Along the road Argostoli–Lixouri (Fig. 2), numerous landslides disrupted the traffic, with the majority in the part between Farsa and Kontogourata, and Agkonas to Myrtos (Fig. 2). Construction and road service teams were working non-stop during the 2 weeks after the Jan. 26 and Feb. 2 events, in order to re-open the road to civilian traffic and repair damages.

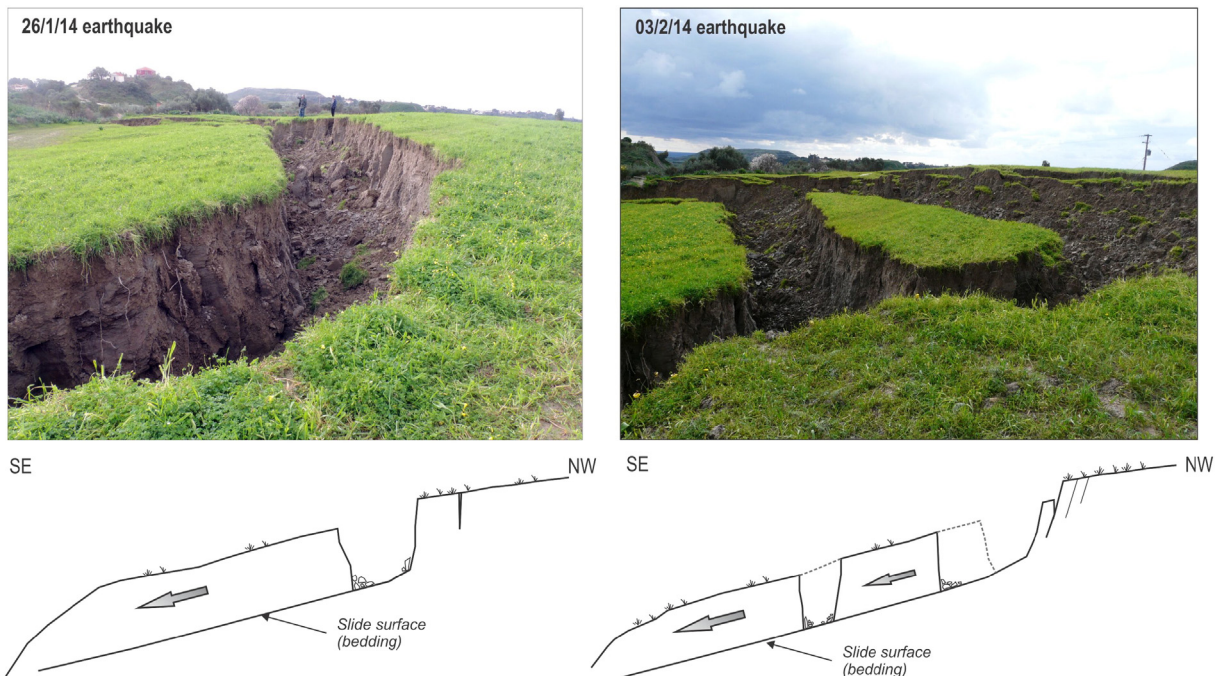


Fig. 5. Field photographs of the large landslide in Soullari village, Paliki Peninsula, Cephalonia. View to the southwest. Sketches below each photograph show a geological interpretation.

2.3. Liquefaction

The most remarkable characteristics of liquefaction phenomena triggered by the 2014 earthquakes are: a) the repeated liquefaction at the same sites within a period of one week (similar phenomena were seen during the Emilia Romagna sequence; Papathanassiou et al., 2012) and b) the boiling of sandy material with gravels in the quay of Lixouri during the second earthquake. Extensive liquefaction was triggered in near-shore extensions of land towards the sea and reclaimed land in the waterfront areas of Argostoli and Lixouri (Fig. 2). Most of the areas affected were those that had been artificially filled after the devastating 1953 earthquakes, a series of three (3) events that totally ruined the majority of houses in the island.

Similar phenomena were triggered by the August 14, 2003 Lefkada earthquake and documented by Papathanassiou et al. (2005). In particular, ejection of sandy material through cracks on the coastal road and the sidewalk and horizontal displacement of the quay walls were mainly reported in the waterfront area of the city of Lefkada. However, the liquefaction-induced damages to port facilities in the area of Lefkada were less severe comparing to the ones triggered by the 2014 Cephalonia earthquakes.

In particular, in the town of Argostoli (Fig. 2), clear evidence of liquefaction occurrence, like sand boils and ground fissures (of variable azimuth) with ejection of silty sand–water mixture, have been triggered by the first and second events according to eyewitnesses and mapped by our team during the post-earthquake field surveys. Settlement of 5–6 cm of the buildings of customs and port authorities was documented and coarse sandy material was ejected from cracks. Similar phenomena were reported at the area of municipality market, in the second quay called “agora”, where sandy material spewed out through existing cracks on the sidewalk and on the pavement along the perimeter of buildings, inducing a vertical displacement of 3–4 cm. Furthermore, typical liquefaction phenomena were documented at the sidewalk area located to the south of the De Bosset bridge, where sandy material ejected through ground cracks. Liquefaction phenomena were also documented in the marina of Argostoli (Fig. 6), an area located at the eastern shore of the bay, and was constructed in 2002 in order to accommodate yachts and boats. In this zone, a large area was covered by grey fine sandy material ejected through ground cracks. The length of the fissures was up to 6 m and their width up to 8 cm. In the same zone, a vertical displacement of the artificial fill that is placed between two piers, from 15 cm to 40 cm, was reported without surface evidence of liquefaction. A characteristic sketch of the liquefied area in marina is shown in Fig. 6, where

the information regarding the orientation, dimensions and spatial distribution of the liquefaction-induced ground disruption is provided.

In the waterfront area of Lixouri (Fig. 7), the liquefaction of the subsoil layers induced severe damages to port facilities and caused the complete loss of functionality for 24 h. In particular, at the area of the building of port authorities, cracks on the sidewalk were opened and brown sandy material was ejected and covered the area of the sidewalk and the park situated behind. Few metres to the south, more than 10 sand craters with diameter up to 50 cm were generated by the second earthquake. At the main quay of Lixouri, at the central part of the waterfront area, sandy material and gravels were ejected indicating the high value of acceleration generated by the second event. These cracks were initially opened during the first earthquake but their width and the amount of ejected material were not so large as those generated during the second earthquake. In the same area, behind the quay walls, large vertical and horizontal displacements were documented, however without any evidence of ejecta.

Scattered liquefaction phenomena were also reported at several locations in Paliki peninsula (Fig. 2): small amount of coarse sandy material ejected through a <2 cm width fissure inside a field located between the villages of Atheras and Livadi; a sand crater with diameter <5 cm was reported in a bank of a stream that crosses Plio-Pleistocene sediments in Soullari; brown coarse sandy material ejected through a crack at the edge of a paved road in Kounopetra (south area of Paliki).

3. Discussion–conclusions

It is of major interest to identify the seismic sources of the Jan.–Feb. 2014 earthquakes and to associate them with the CTF itself or not. To associate our field observations with CTF or other active faults beneath Paliki peninsula, we need to use seismological data as no fault surface breaks were identified during our field surveys. So, we used the right-lateral nodal plane from focal mechanisms for the event of Jan. 26, 2014 (<http://bbnet.gein.noa.gr/HL/seismicity/moment-tensors>) published by NOA and other organisations, together with the relocated epicentres published in the NOA web report http://www.gein.noa.gr/Documents/pdf/ekthesi_G_I_26-2-2014_v2.pdf. Then, we projected the Jan. 26, 2014 right-lateral fault plane to the surface (Fig. 3A) using magnitude–surface length empirical relationships from Wells and Coppersmith (1994; Fig. 3A, red line with arrows on either side). The Feb. 3, 2014 fault plane could not be unequivocally projected as most focal mechanisms suggest a north–south striking, nearly-vertical, strike-slip fault plane while there is one solution (GFZ; published on

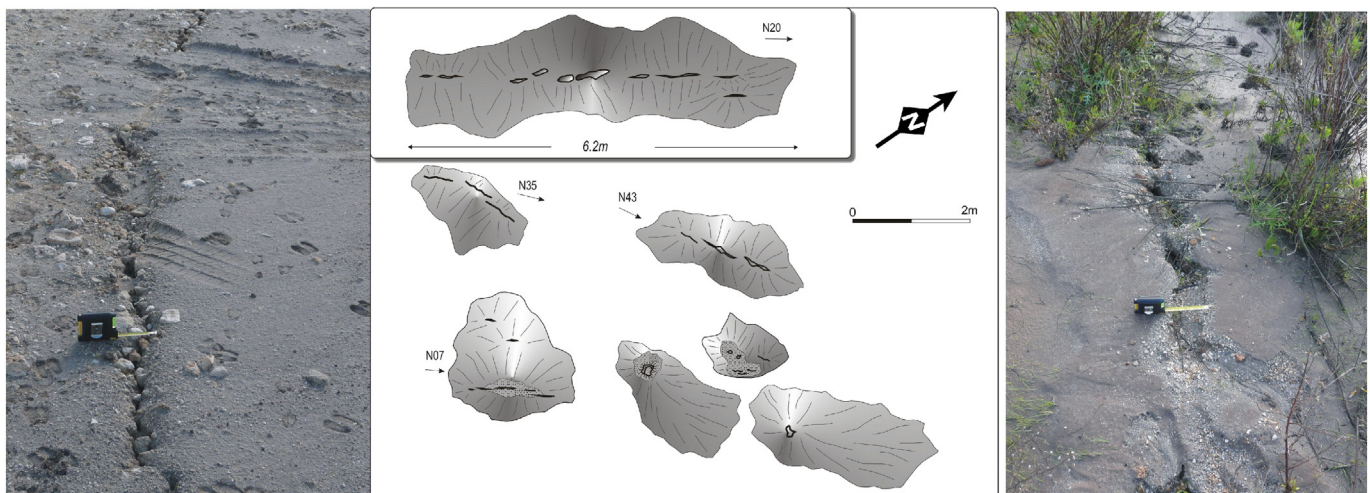


Fig. 6. Field photographs (taken on Feb. 8, 2014) of liquefaction phenomena, triggered in the area of Argostoli marina (see map in Fig. 2). A characteristic sketch of liquefaction surface evidence (arrows indicate fissure azimuth; in general NE–SW) is showing in the middle (notice scale bar in metres).



Fig. 7. Map showing the liquefaction manifestation (black star), the cracks/fissures along the waterfront area and the location of buckling phenomena in the town of Lixouri. In addition, characteristic liquefaction-induced structural damages are shown in post-Feb 3, 2014 field photographs (photos taken on Feb. 7, 2014) on the right and particularly a broken water pipeline due to the sloshing of the ground (top), a “graben” formation behind quay wall (middle) and movement of the quay wall towards the sea (bottom).

line at <http://www.emsc-csem.org/Earthquake/mtfull.php?id=357329>) pointing to a west-dipping fault. Nevertheless, it is expected that both fault lengths to be in the range 10–12 km based on empirical relationships of Wells and Coppersmith (1994). The available, preliminary data indicate the activation of two sub-parallel, possibly-overlapping strike-slip faults beneath Paliki Peninsula. This two-fault pattern stays the same if epicentre location errors of 1-km and/or errors of 5-degree fault-dip angle are allowed. We note that the second event was shallower (by comparing NOA MT centroids) and the rupture may have sporadically reached the surface due to the abundance of surface cracks in north Paliki peninsula (co-seismic fractures? Figs. 2, 3, 4).

The Jan.–Feb 2014 earthquakes highlighted the need for more seismological and geophysical data acquisition offshore Cephalonia, to locate CTF and map its structure (one segment or several; dip directions

and dip angles). Previous work from seismic profiles (Kokinou et al., 2005; Sachpazi et al., 2000) locate the CTF within 10-km to the west of Cephalonia, however 20-th century seismicity runs along Cephalonia’s west coast. It still remains an open question if CTF is actually running along the Cephalonia west coast or it is a system of offshore & onshore fault zones of 10?-km long overlapping segments.

Both earthquakes generated strong ground motions that were recorded on the installed accelerographs in the island. Regarding the first event, Jan. 26, 2014 the accelerographs installed in Argostoli by EPPO-ITSACK recorded a peak ground acceleration (PGA) value (horizontal component) equal to 383.4 cm/sec^2 (EPPO-ITSACK, 2014a; <http://www.itsak.gr/news/news/64>) while the accelerograph installed in Lixouri by NOA recorded a PGA value equal to 531 cm/sec^2 (Kalogeras, 2014). In both cases, it is obvious that this high ground motion is the

triggering factor of the liquefaction-induced damages. The second event, Feb. 3, 2014 caused severe damages mainly in Paliki and less damages in the area of Argostoli. According to the records of the accelerographs installed by EPPO-ITSAK in Chavriata (CHV1; see location Habriata in Figs. 2 and 3), Lixouri (LXR1) and ARG2 (Argostoli) the PGA values were equal to 752 cm/sec², 667 cm/sec² and 264 cm/sec², respectively (EPPO-ITSAK, 2014b). Thus, taking into account these values, it can be assumed that the ejection of gravels in the waterfront area of Lixouri is the outcome of the generation of high excess pore pressure due to the strong ground motion. In addition, the fact that the second event triggered more ground failures in the Paliki peninsula in comparison to the central and eastern parts of Cephalonia can be explained by the differences in the recorded PGA values in Paliki peninsula and Argostoli, respectively.

An important result of our work comprises that most of the coastal areas severely affected were those that had been artificially filled after the devastating 1953 earthquakes. The material used to reclaim devastated areas due to the 1953 earthquakes was not appropriate. This must be taken into account by geotechnical experts, engineering geologists and civil engineers in future works.

Acknowledgements

We thank Efthimios Lekkas, Gerassimos Papadopoulos, Ioannis Koukouvelas, Spiros Pavlides, Alexandros Chatzipetros, Ioannis Kassaras, Vassilios Karastathis, Nikos Theodoulidis, Ioannis Kalogeras, Alexandra Moshou and Maria Sachpazi for discussions. We appreciate detailed review comments by Eugenie Perouse and one anonymous reviewer. We thank Laurent Jolivet for editorial assistance. Fieldwork was funded by the GSRT (Grant number 12CHN124) project INDES-MUSA <http://www.indes-musa.gr/> and the FP7 (Grant number 606888 / FP7-SPACE-2013-1) project RASOR <http://www.rasor-project.eu/>. We are indebted to the local authorities for permits and assistance. A .kml file with all the field observations (Table 1) is available in Suppl. material.

Appendix A. Supplementary data

Supplementary data associated with this article can be found in the online version, at <http://dx.doi.org/10.1016/j.tecto.2014.05.012>. These data include Google maps of the most important areas described in this article.

References

- EPPO-ITSAK, 2014a. The January 26th, 2014 Earthquake in Cephalonia, Preliminary Report, by EPPO-ITSAK (in Greek). (<http://www.slideshare.net/itsak-eppo/2014-0127-kefaloniaeqpreliminaryreporta>).
- EPPO-ITSAK, 2014b. Strong Ground Motion of the February 3, 2014 Cephalonia Earthquake: Effect on Soil and Built Environment in Combination with the January 26, 2014 Event. (<http://www.slideshare.net/itsak-eppo/20140203-kefaloniaeq-report-en>).
- Ganas, A., Marinou, A., Anastasiou, D., Paradissis, D., Papazissi, K., Tzavaras, P., Drakatos, G., 2013a. GPS-derived estimates of crustal deformation in the central and north Ionian Sea, Greece: 3-yr results from NOANET continuous network data. *J. Geodyn.* 67, 62–71.
- Ganas, A., Oikonomou, A.I., Tsimi, Ch., 2013b. NOFAULTS: a digital database for active faults in Greece. *Bull. Geol. Soc. Greece XLVI* (Online version at <http://194.177.194.115/panearth/mapfix.html>).
- Ganas, A., F. Cannavò, P.J. González and G. Drakatos, 2014. The geodetic signature of the Jan 26, 2014 earthquake onshore Cephalonia, Greece, unpublished report http://www.gein.noa.gr/Documents/pdf/VLSM_co-seismic_26-1-2014_13_55_UTC.pdf.
- Hollenstein, C., Müller, M.D., Geiger, A., Kahle, H.-G., 2008. Crustal motion and deformation in Greece from a decade of GPS measurements, 1993–2003. *Tectonophysics* 449 (1–4), 17–40. <http://dx.doi.org/10.1016/j.tecto.2007.12.006>.
- NOA web report, 2014, unpublished, http://www.gein.noa.gr/Documents/pdf/Kefalonia2014_ekthesi_G_I.pdf, last accessed May 19, 2014.
- Kalogeras, I., 2014. Preliminary Analysis of the Recorded Strong Ground Motion Triggered by the January 26, 2014 Cephalonia Earthquake. (in Greek) (Available on-line at http://www.gein.noa.gr/Documents/pdf/Cefalonia_20140126_preliminary_web.pdf).
- Karastathis, V., Koukouvelas, I., Ganas, A., Moschou, A., Mouzakiotis, A., Papadopoulos, G.A., Spanos, D., 2014. The strong M_w 6 earthquake of 26th January 2014 in Cephalonia island, Ionian Sea, Greece: a first report. *Geophys. Res. Abstr.* 16 (EGU2014-17001).
- Kokinou, E., Kamberis, E., Vafidis, A., Monopolis, D., Ananiadis, G., Zelelidis, A., 2005. Deep seismic reflection data Greece: a new crustal model for the Ionian sea. *J. Pet. Geol.* 28 (2), 81–98.
- Lekkas, E., Danamos, G., Mavrikas, G., 2001. Geological structure and evolution of Cephalonia and Ithaki Islands. *Bull. Geol. Soc. Greece XXXIV/1*, 11–17.
- Louvari, E., Kiratzi, A.A., Papazachos, B.C., 1999. The CTF and its extension to western Lefkada Island. *Tectonophysics* 308, 223–236.
- Papathanassiou, G., Pavlides, S., Ganas, A., 2005. The 2003 Lefkada earthquake: field observations and preliminary microzonation map based on liquefaction potential index for the town of Lefkada. *Eng. Geol.* 82, 12–31.
- Papathanassiou, G., Caputo, R., Rapti-Caputo, D., 2012. Liquefaction phenomena along the palaeo-Reno River caused by the May 20, 2012 Emilia (Northern Italy earthquake). *Ann. Geophys.* 55 (4), 735–742.
- Pérouse, E., Chamot-Rooke, N., Rabaute, A., Briole, P., Jouanne, F., Georgiev, I., Dimitrov, D., 2012. Bridging onshore and offshore present-day kinematics of Central and Eastern Mediterranean: implications for crustal dynamics and mantle flow. *Geochim. Geophys. Geosyst.* 13, Q09013.
- Sachpazi, M., et al., 2000. Western Hellenic subduction and Cephalonia Transform: local earthquakes and plate transport and strain. *Tectonophysics* 319, 301–319.
- Scordilis, E.M., Karakaisis, G.F., Karakostas, B.G., Panagiotopoulos, D.G., Cominakis, P.E., Papazachos, B.C., 1985. Evidence for transform faulting in the Ionian Sea: the Cephalonia Island earthquake sequence of 1983. *Pure Appl. Geophys.* 123, 388–397.
- Wells, D.L., Coppersmith, J.K., 1994. New empirical relationships among magnitude, rupture length, rupture width, rupture area, and surface displacement. *Bull. Seismol. Soc. Am.* 84, 974–1002.